Available online at www.sciencedirect.com
SCIENCE DIRECT®
Electrochimica Acta 50 (2005) 4444–4450
ELECTROCHIMICA Acta
www.elsevier.com/locate/electacta

Two-equivalent electrochemical reduction of a cyano-complex $[Tl^{III}(CN)_2]^+$ and the novel di-nuclear compound $[(CN)_5Pt^{II}-Tl^{III}]^0$

Tina D. Dolidze [a], Dimitri E. Khoshtariya [a,b,*], Mårtin Behm [c], Göran Lindbergh [c], Julius Glaser [d,**]

[a] Institute of Inorganic Chemistry and Electrochemistry, Georgian Academy of Sciences, Jikiya 7, Tbilisi 0186, Georgia
[b] Institute of Molecular Biology and Biophysics, Georgian Academy of Sciences, Gotua 14, Tbilisi 0160, Georgia
[c] Department of Applied Electrochemistry, The Royal Institute of Technology (KTH), S-10044 Stockholm, Sweden
[d] Department of Inorganic Chemistry, The Royal Institute of Technology (KTH), S-10044 Stockholm, Sweden

Received 22 June 2004; received in revised form 29 November 2004; accepted 6 February 2005
Available online 2 March 2005

Abstract

Extending our recent insights in two-electron transfer microscopic mechanisms for a Tl^{III}/Tl^{I} redox system [D.E. Khoshtariya, et al., Inorg. Chem. 41 (2002) 1728], the electrochemical response of glassy carbon electrode in acidified solutions of Tl^{III} $(ClO_4)_3$ containing different concentrations of sodium cyanide has been extensively studied for the first time by use of cyclic voltammetry and the CVSIM curve simulation PC program. The complex $[Tl^{III}(CN)_2]^+$ has been thoroughly identified electrochemically and shown to display a single well-defined reduction wave (which has no anodic counterpart), ascribed to the two-equivalent process yielding $[Tl^{I}(aq)]^+$. This behavior is similar to that of $[Tl^{III}(aq)]^{3+}$ ion in the absence of sodium cyanide, disclosed in the previous work, and is compatible with the quasi-simultaneous yet sequential two-electron transfer pattern (with two reduction waves merged in one), implying the rate-determining first electron transfer step (resulting in the formation of a covalently interacting di-thallium complex as a metastable intermediate), and the fast second electron transfer step. Some preliminary studies of the two-equivalent reduction of directly metal–metal bonded stable compound $[(CN)_5Pt^{II}–Tl^{III}]^0$ has been also performed displaying two reduction waves compatible with a true sequential pattern.
© 2005 Elsevier Ltd. All rights reserved.

Keywords: Thallium(III); Cyano-complexes; Two-electron transfer; Cyclic voltammetry; Di-nuclear complexes

1. Introduction

The diverse mechanisms of multi-electron transfer are of fundamental interest due to their significant, not fully recognized, role in biological and chemical processes [1–4]. However, notwithstanding the significant progress in their theoretical understanding [5–7], the number of even well-characterized two-electron transfer processes is much smaller compared with that of corresponding single-electron processes. In particular, despite some earlier efforts, the two-equivalent redox chemistry of thallium(III) is rich in various unresolved puzzles. Both homogeneous and electrode processes of aqueous complex $[Tl^{III}(aq)]^{3+}$ have been studied in the past (see Refs. [8–11] and references sited therein). Thallium(III) is known to form very strong complexes of different ligand compositions, in particular with CN^-, while thalliun(II) and thallium(I) do not [8,9,12,13]. The homogeneous systems containing cyanide ions were investigated in the context of the electron exchange kinetics [8] and the ligand uptake stability constants [9]. However, electrochemical studies of thallium(III) cyano-complexes have not been performed so far.

In our previous work [11] we accomplished the detailed study of electrochemical two-equivalent reduction of $[Tl^{III}(aq)]^{3+}$ to $[Tl^{I}(aq)]^+$ in acidified solutions of sodium per-

* Corresponding author. Tel.: +7 995 32 386077; fax: +7 995 32 939157.
** Co-corresponding author.
E-mail addresses: dimitri.k@joker.ge (D.E. Khoshtariya), julius@inorg.kth.se (J. Glaser).

0013-4686/$ – see front matter © 2005 Elsevier Ltd. All rights reserved.
doi:10.1016/j.electacta.2005.02.006

chlorate containing different concentrations of $Tl^{III}(ClO_4)_3$. On the basis of experimental results, obtained by use of cyclic voltammetry (CV) and rotating disk electrode (RDE) techniques, and the subsequent data analysis by the curve simulation PC program (CVSIM) [14], it has been suggested that this two-equivalent reduction process occurs through the quasi-simultaneous sequential mechanism, probably via formation of covalently interacting (yet unstable) di-thallium(II) intermediate [11]. The overall reaction involves three steps, viz.:

$$2\,[Tl^{III}(aq)]^{3+} + 2e^- \Rightarrow 2[Tl^{II}(aq)]^{2+} \quad \text{(slow)} \tag{1}$$

$$2[Tl^{II}(aq)]^{2+} \Rightarrow [Tl^{II}\text{–}Tl^{II}]^{4+} \quad \text{(fast)} \tag{2}$$

$$[Tl^{II}\text{–}Tl^{II}]^{4+} + 2e^- \Rightarrow 2[Tl^{I}(aq)]^{+} \quad \text{(fast)} \tag{3}$$

This pattern, showing up in a single (merged) reduction wave, results from the facts that: (1) the $[Tl^{II}]^{2+}$ ion (whatever set of redox potentials for individual steps is chosen, see Ref. [11]) is a stronger oxidant than $[Tl^{III}]^{3+}$ [9–11]; (2) according to the solid-state structural data [15,16], there should exist at least the 6s–6s bonding interaction between the Tl^{II} species [11], by the analogy with two relative iso-electronic systems, Au^0–Au^0 and Hg^I–Hg^I [17,18].

The aim of the present work was an essential extension of our previous studies of aqueous thallium(III) ($[Tl(aq)]^{3+}$) electrochemistry [11]. In particular, (a) an electrochemical identification of thallium(III) cyano-complexes, and the novel di-nuclear compound $[(CN)_5Pt^{II}-Tl^{III}]^0$, disclosed in earlier work mostly by the multinuclear NMR techniques (see Refs. [13] and [19,20], respectively), and (b) detailed study of electrochemical mechanisms for two-equivalent reduction for these compounds in comparison with the mechanism of aqueous thallium(III) investigated earlier [11].

2. Experimental

The electrochemical experiments were carried out on a PAR 273 Potentiostat/Galvanostat, controlled by EG&G Model Software. Two kinds of cells with standard three-electrode configurations containing 50 and 5 ml of working solution were used. Glassy carbon working electrodes (areas 0.1256 and 0.0314 cm^2) were cleaned before each series of experiments by polishing with 1.0; 0.3; and 0.05 μm aluminum granules from Buehler on the Buehler polishing cloth, followed by sonification in purified water (vide infra). The saturated calomel reference electrode and/or a silver/silver chloride reference electrodes were separated from the main cell by glass frits. All potentials quoted in this paper are refered to a normal hydrogen electrode (NHE). Measurements were performed at room temperature (24 ± 1) °C.

Working solutions were prepared from the stock solution of $Tl^{III}(ClO_4)_3$ using aqueous solution of $HClO_4$ or aqueous acidified solution of $NaClO_4$ by adding of appropriate amounts of NaCN. Stock solution [1.02 M $Tl^{III}(ClO_4)_3$ + 7.28 M $HClO_4$ + $Tl^{I}ClO_4$, latter unavoidably present as an impurity (≤1%)] was prepared according to the procedure described earlier [21]. Ultrapure water was supplied by a Millipore Milli-Q system. Synthesis of the solid compound $[(CN)_5Pt^{II}-Tl^{III}]^0$ also described elsewhere [20]. All other chemicals used were commercial products of highest purity available. Computer simulation procedures were run using CVSIM Program [14].

3. Results and discussion

3.1. Overview (including data for a $[Tl^I(aq)]^+/Tl^0$ couple)

Typical CV experiments (at scan rates covering the range of 0.01–0.5 V/s) were performed for working solutions containing $Tl^{III}(ClO_4)_3$ at 2×10^{-3} to 5×10^{-2} M, $Tl^{I}ClO_4$ at ca. 2×10^{-5} to 5×10^{-4} M, without (see Ref. [11]) or with the addition of 0.025–0.05 M NaCN, within the broad potential range of +2.5 to −0.8 V (most experiments were run within +1.2 to −0.5 V). Under these conditions, within the potential range of +1.0 to −0.5 V, voltammograms exhibited a single reduction wave, peaked at ca. +0.75 V (in the absence of NaCN), or at ca. +0.05 V (in the presence of NaCN), Fig. 1, attributable to the reduction of Tl^{III} species present in two different coordination forms (vide infra). No anodic counterpart for either of these waves (within the whole potential range extended up to +2.5 V) was observed on the reverse scan in both cases. However, when the potential range was extended down to −0.8 V, the reduction and oxidation waves peaked at −0.6 and −0.4 V, respectively, could be observed (Fig. 2), attributable to the $[Tl^{I}(aq)]^+/Tl^0$ couple [10]. Fig. 2 simultaneously represents CV curves for both, the $[Tl^{III}(aq)]^{3+}/[Tl^{I}(aq)]^+$ and $Tl^{I}(aq)]^+/Tl^0$ couples for the solution initially containing only ca. 1% of Tl^I compared to

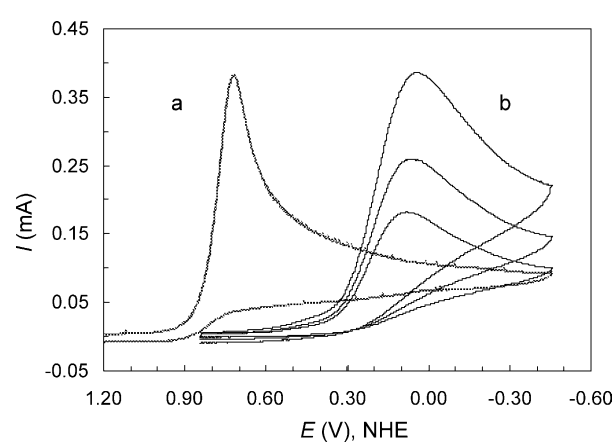

Fig. 1. Cyclic voltammograms for glassy carbon electrode (area: 0.1256 cm^2): (a) 1 M $NaClO_4$ + 0.273 M $HClO_4$ + 0.01 M $Tl(ClO_4)_3$ at scan rate $v = 0.1\ V\,s^{-1}$, and (b) in1 M $NaClO_4$ + 0.073 M $HClO_4$ + 0.01 M $Tl(ClO_4)_3$ + 0.025 M NaCN at the scan rates (from top to bottom) 0.2, 0.1 and 0.05 $V\,s^{-1}$, respectively.

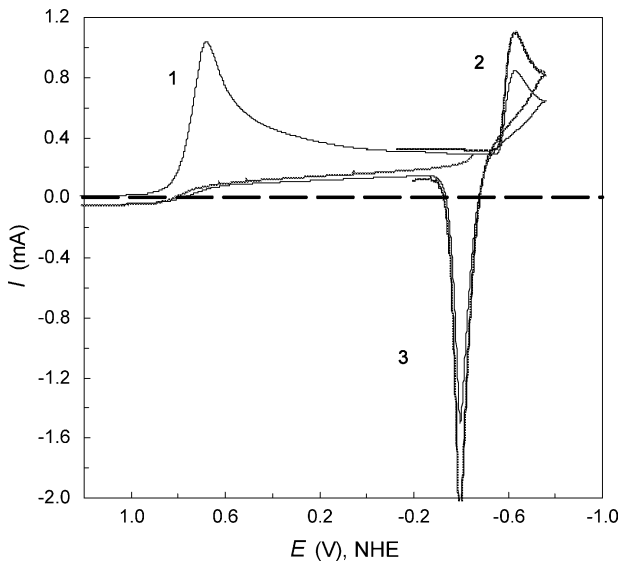

Fig. 2. Simultaneous representation of CV curves for the $[Tl^{III}]^{3+}/[Tl^{I}]^{+}$ (reduction wave is numbered as 1) and $[Tl^{I}]^{+}/Tl^{0}$ (reduction and oxidation waves numbered as 2 and 3, respectively) couples (glassy carbon electrode, area: 0.1256 cm^2, scan rate: 0.5 V s^{-1}) in solution containing 1 M $HClO_4$ + 0.01 M $Tl^{III}(ClO_4)_3$ + 0.0001 M $Tl^{I}ClO_4$. Solid curve: total first scan; thin curve 1 represents the early return path for the first wave; thin curves 2 and 3 represent the total sixth scan. See Sections 3.1 and 3.2 for further details.

Tl^{III}. The intensity of both the reduction and oxidation waves for the latter couple increases with the increase of Tl^{I} concentration (caused either by beforehand electrochemical reduction of Tl^{III}, or by simple adding of $TlClO_4$ to the solution, see Fig. 2), and exhibits the shape (an abrupt current rise and a loop) typical for metal deposition reaction due to the nucleation overpotential. At the same time, the oxidation wave is sharp and symmetrical, indicating that reactant is deposited on the electrode (see, e.g., Ref. [22] and fig. 6.24 therein). This couple, which starting component, Tl^{I}, initially maintained at the concentration of ca. 1% (subsequently increasing as a result of electrochemical reduction of Tl^{III}, Fig. 2), has been used in some further experiments as an internal marker (vide infra). An observation that the magnitudes of peak currents for the $[Tl^{I}(aq)]^{+}/Tl^{0}$ couple present as an impurity are comparable to the one for the reduction of the main component (Tl^{III}, coordinated either with water or CN^{-}, respectively, Figs. 1 and 2) can be readily explained by different intrinsic charge-transfer mechanisms behind these CV waves (numbered by 1–3 in Fig. 2). In particular, wave 1 represents outer-sphere electron transfer in the course of the reduction of freely diffusing Tl^{III} species (vide infra), whereas waves 2 and 3 probably represent the intrinsic steps of reduction (complete discharge of weakly adsorbed Tl^{I} that follows the preceding ion transfer step, see Refs. [6,22]), and oxidation of the deposited Tl^{0} that can be considered as strongly adsorbed particle [22]. Consequently, the cases of CV waves 2 and 3, in contrast with wave 1 in which case the peak current is given by Eq. (6) (see the next sub-section below) these peak currents are proportional to surface concentrations of weakly adsorbed and deposited species, respectively, and, hence are not directly comparable with each other regarding the actual bulk concentrations of two kinds of reactant ions under the comparison.

3.2. Reduction of $[Tl^{III}(aq)]^{3+}$ [11]

The overall electrochemical mechanism for this two-equivalent process has been thoroughly analyzed in the previous work [11]. The RDE technique, along with the CV voltammetry, latter furnished by the extended CV curve simulation procedure (CVSIM Program [14]), were applied towards the elucidation of the microscopic two-equivalent pattern. In brief, theoretical analysis (cross-testing) included the following procedures (this analysis turned to be equally valid also for the branch case of the two-equivalent $[Tl^{III}(CN)_2]^{+}$ reduction, see Section 3.3):

1. Application of basic general Eqs. (4)–(7) valid for irreversible electrochemical processes [22–24]:

$$E_p - E_{(p/2)} = \frac{47.7}{\alpha n_\alpha} \quad (\text{mV}), \tag{4}$$

$$(E_p)_1 - (E_p)_2 = \frac{RT}{\alpha n_\alpha F} \ln\left(\frac{v_1}{v_2}\right)^{1/2} \tag{5}$$

$$I_p = 2.99 \times 10^5 n(\alpha n_\alpha)^{1/2} A c_0 D^{1/2} v^{1/2} \tag{6}$$

$$k_1^0 = \frac{4.405 I_p}{nFAc_0 \exp[(-\alpha n_\alpha F/RT)(E_1^0 - E_p)]} \tag{7}$$

where E_p is the peak potential, and $E_{p/2}$ is the half peak potential, α is the transfer coefficient, n_α is the number of electrons transferred in the rate-determining step, n is the total number of electrochemically transferred electrons, A is the area of working electrode and c_0 is the reactant's bulk concentration, v is the scan rate, I_p is the peak current, E_1^0 is the standard potential for the rate-determining (here first) electron transfer step, and k_1^0 is the standard rate constant for the same step, T is the absolute temperature, R and F are the gas and Faraday constants, respectively. The following observations were essential: the plot of peak current as a function of square root of the scan rate, is linear and passes through the origin (Fig. 3). The peak potential is shifting to the negative potentials with increase of the scan rate, but a bias for the half peak potential shift remains constant.

Also, the invariance of ratios $I_p/v^{1/2}$ and $\Delta E_{p/2}/\Delta \lg v$ over the entire range of scan rates applied indicate that chemical (e.g. dismutatio/disproportionation) reactions does not alter kinetic aspects of the electrode (rate-determining) process [11,22,23]. Eqs. (4) and (5), as well as the Tafel equation applied to the RDE data (Ref. [11]), allowed for the direct determination of the value for a product αn_α. Furthermore, after setting of a realistic value for D (of two possible choices), Eqs. (4)–(6) allow for the direct and unequivocal determination of the following values: $n = 2$, $n_\alpha = 1$, $\alpha = 0.66$, Table 1. This set of parameters

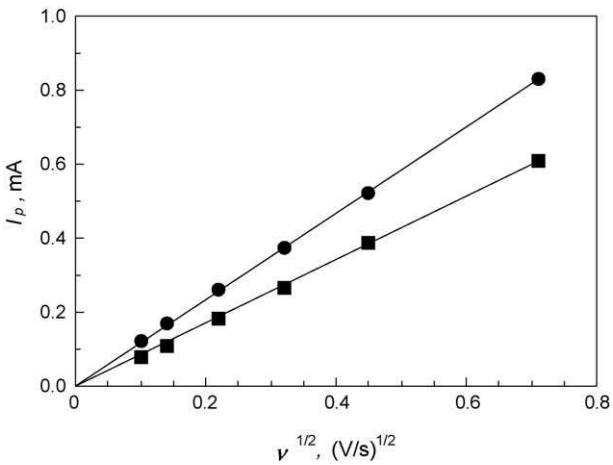

Fig. 3. Dependence of peak current of cyclic voltammograms for glassy carbon electrode on the square root of scan rate in the solutions of (●) 1 M $NaClO_4$ + 0.273 M $HClO_4$ + 0.01 M $Tl(ClO_4)_3$, and (■) the same solution, after addition of 0.05 M NaCN.

indicates that both electrons are transferred electrochemically, and that the rate-determining step includes transfer of one electron. In addition, a value of E_1^0 has been roughly determined from the visual analysis of CV curves, allowing for a rough determination of k_1^0 according to Eq. (7), Table 1. However, a transfer of the second electron cannot be considered as an independent process, since the Tl^{2+} ion is a stronger oxidant than Tl^{3+}. This case is considered in the literature to be characterized by a single (merged) wave, the peak current of which is determined by two electron equivalents, and the shape of which is determined by the parameters (α_1, E_1^0, k_1^0) of the first electron transfer step in the sequence [11,22,24].

2. Application of the CVSIM Program. Computer simulation by the CVSIM Program (based on the explicit finite difference method) has been proven to be a powerful tool for the analysis of CV experiments. The shape of a CV curve reflects the intrinsic features of all the stages, including the interface charge transfer and solution chemical reactions (that are coupled to the charge transfer), contributing to the overall process. Thus, through the CV study, normally one can deduce a great deal of information regarding the constituent stages. Simulations can be very helpful, both in the preliminary stages of CV studies (in deciding the general mechanism)and in the extraction of rate and equilibrium parameters of the chosen mechanism by comparing experimental CV curves with those successively generated by the program. The CVSIM Program embodies all the accumulated knowledge on the electrochemical mechanisms collected up to early nineteen nineties, including the multi-electron mechanisms, and enables one to generate CV curves for nearly any desired mechanism and any realistic sets of intrinsic parameter [14] (see also Ref. [25] for the related information).

Assuming the above deduced mechanism of two-electron reduction for the aqueous $[Tl^{III}(aq)]^{3+}$ species (as well as $[Tl^{III}(CN)_2]^+$ species to be considered below), and using the estimated values of α_1, E_1^0, k_1^0, n and n_α, as starting values for the simulation program, the other constituent values, viz., α_2, k_1^0, k_2^0, were smoothly varied within the reasonable ranges, aiming the reproduction of experimental CV curves at the maximal accuracy. Further iterative steps included slight (adjusting) variation of the values for "known" parameters, α_1, E_1^0 and k_1^0 such to achieve the desirable coincidence of simulated and experimental CV curves. As a result, the experimental curves were surprisingly well reproduced by the values of α_1, E_1^0 and k_1^0 that felt within rather narrow ranges very close to the corresponding initial values (Fig. 4, Tables 1 and 2). We note that the decrease of the simulated value for E_1^0 cor-

Table 1
Kinetic parameters estimated through the cross-testing analysis of experimental data for two-equivalent reduction of $[Tl^{III}(aq)]^{3+}$ and $[Tl^{III}(CN)_2]^+$ (see text for details)

Reactant	Technique	α_1	D ($\times 10^6$ cm^2 s^{-1})	lg(k_1^0) (cm s^{-1})	E_1^0 (V)
$[Tl^{III}(aq)]^{3+}$ *	CV **	0.66 ± 0.04	3.72 ± 0.32	−5.4 ± 0.3	1.04
$[Tl^{III}(aq)]^{3+}$ *	RDE	0.65 ± 0.01	3.52 ± 0.10	−5.5 ± 0.1	1.04
$[Tl^{III}(CN)_2]^+$ ***	CV **	0.33 ± 0.03	3.32 ± 0.30	−6.4 ± 0.6	0.89

* Data from Ref. [11].
** Estimates based on Eqs. (4)–(7).
*** This work.

Table 2
CVSIM simulation results (for CV curves) for two-equivalent reduction of $[Tl^{III}(aq)]^{3+}$ and $[Tl^{III}(CN)_2]^+$ (see text for details)

Reactant	E_1^0 (V)	E_2^0 (V)	lg(k_1^0) (cm s^{-1})	lg(k_2^0) (cm s^{-1}) **	α_1	α_2 **
$[Tl^{III}(aq)]^{3+}$ *	1.04 ± 0.1	1.46 ***	−5.7 ± 0.6	−5.4 ± 1.2	0.65 ± 0.05	0.5 ± 0.2
$[Tl^{III}(CN)_2]^+$	0.89 ± 0.1	1.46	−6.5 ± 0.6	−5.4 ± 1.2	0.35 ± 0.05	0.5 ± 0.2

* Data from Ref. [11].
** Rough estimates.
*** Estimated by using the equation $E^0 = (E_1^0 + E_2^0)/2 = 1.25$ V [10].

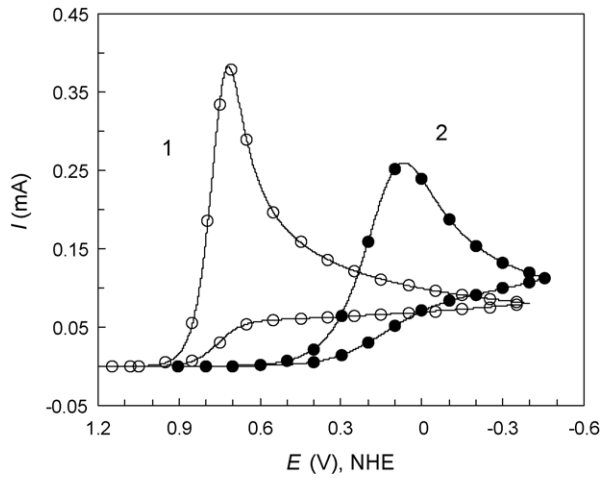

Fig. 4. Experimental data of Fig. 1 both at scan rate of $v = 0.1\,\mathrm{V\,s^{-1}}$: solid curves (after minor background corrections). Curve a: reduction of $[Tl^{III}(aq)]^{3+}$; curve b: reduction of $[Tl^{III}(CN)_2]^+$. Simulated CV curves. (1) Open circles: $n = 2$, $n_\alpha = 1$, $E_1^0 = 1.04\,\mathrm{V}$, $\alpha_1 = 0.65$, $k_1^0 = 2 \times 10^{-6}\,\mathrm{cm\,s^{-1}}$, $E_2^0 = 1.46\,\mathrm{V}$, $\alpha_2 = 0.5$, $k_2^0 = 2 \times 10^{-6}\,\mathrm{cm\,s^{-1}}$; (2) filled circles: $n = 2$, $n_\alpha = 1$, $E_1^0 = 0.89$, $\alpha_1 = 0.3$, $k_1^0 = 3 \times 10^{-7}\,\mathrm{cm\,s^{-1}}$, $E_2^0 = 1.46\,\mathrm{V}$, $\alpha_2 = 0.5$, $k_2^0 = 2 \times 10^{-6}\,\mathrm{cm\,s^{-1}}$.

relates with the increase of the corresponding value of k_1^0 within these narrow ranges indicated in Table 2. The parameters characterizing the second electron transfer step were fixed with much lower exactness (Table 2). This is due to the fact that the shapes of CV waves are much less affected by the intrinsic kinetic characteristics of the second electron transfer step. However, the peak current is affected equally by both the steps [26].

3.3. Two-electron reduction of $[Tl^{III}(CN)_2]^+$

Upon the addition of $0.025 \div 0.05\,\mathrm{M}$ NaCN to working solutions containing $Tl^{III}(ClO_4)_3$ at 2×10^{-3} to $5 \times 10^{-2}\,\mathrm{M}$, the above discussed two-electron reduction wave peaked at ca. +0.75 V, is shifted to +0.05 V (Fig. 1a and b, respectively). No sign of the former $[Tl^{III}(aq)]^{3+}$ reduction wave remains on the CV scan. The shape of a "new" wave is different from the original one. However, the peak current again changes linearly as a function of square root of the scan rate (Fig. 3). All these fact are indicative of Tl^{III} complexation by the CN^- ions according to the results of former NMR studies [13]. The previous detailed computer analysis of systematic NMR data, using the PC Program "Medusa", allowed for the calculations of concentrations for different kind of thallium(III) cyanocomplexes at different solution compositions (concentrations of solution components such as Tl^{III}, CN^-, H^+). According to the previous results [13], verified also by the new calculations, under the specified range of CN^- concentrations, almost 100% of Tl^{III} is present as the species: $[Tl^{III}(CN)_2]^+$. Hence, the newly detected reduction wave should be ascribed to this complex ion (vide infra).

Our further analysis of the two-equivalent electrochemical pattern for the $[Tl^{III}(CN)_2]^+$ complex ion is based on two reasonable assumptions:

(a) The overall general mechanism deduced earlier for aqueous thallium(III) species, $[Tl^{III}(aq)]^{3+}$, does not change upon the complexation with two CN^- ligands (leading to the $[Tl^{III}(CN)_2]^+$ species acting as a main component instead if $[Tl^{III}(aq)]^{3+}$).
(b) The $[Tl^{III}(CN)_2]^+$ ions lose both cyano-ligands through the first electron transfer step, because the intermediate (Tl^{II}) and product (Tl^{I}) species are known to be inert regarding such a complexation [8,12,13].

Hence, the overall two-equivalent pattern can be presented as:

$$2\,[Tl^{III}(CN)_2]^+ + 2e^- \Rightarrow 2[Tl^{II}(aq)]^{2+} + 4CN^- \quad \text{(slow)} \tag{8}$$

$$2\,[Tl^{II}(aq)]^{2+} \Rightarrow [Tl^{II}\text{–}Tl^{II}]^{4+} \quad \text{(fast)} \tag{9}$$

$$[Tl^{II}\text{–}Tl^{II}]^{4+} + 2e^- \Rightarrow 2\,[Tl^{I}(aq)]^+ \quad \text{(fast)} \tag{10}$$

where steps (9) and (10) probably are identical to steps (2) and (3) for the reduction of $[Tl^{III}(aq)]^{3+}$ in the absence of NaCN.

The peak shift observed for the cyano-complex ion $[Tl^{III}(CN)_2]^+$ (Fig. 1), generally may be due to the changes of all three major parameters α_1, k_1^0 and E_1^0 of the first slow electron transfer step. The cross-testing analysis procedure, including steps (1) and (2) described in the previous sub-section, has been applied to the CV data ascribed to the $[Tl^{III}(CN)_2]^+$ species completely. The values of basic parameters obtained from the theoretical analysis through Eqs. (4)–(7), and through the CVSIM simulation, are presented in Tables 1 and 2, respectively. We found that the change of α_1 from 0.66 to 0.33 is mainly responsible for the change of the peak shape, and can be only in part responsible for the observed peak shift. Another contribution comes from the change of the value of E_1^0 from 1.04 to ca. 0.89 V (Tables 1 and 2). Note that as in the case of $[Tl^{III}(aq)]^{3+}$, in the course of the reduction of $[Tl^{III}(CN)_2]^+$, we could not observe individual waves for the first and second electro-reduction steps, but only a single well-defined reduction wave. Evidently, in both cases the metastable intermediate containing the $[Tl^{II}]^{2+}$ ion(s) is a stronger oxidant than Tl^{III} (complexed or uncomplexed with the cyanide), $E_2^0 > E_1^0$ [9–11]. Under this condition, if the potential separation between successive reductions is more than 180 mV (second electron transfer is easier, e.g. takes place at more positive potentials than first step), the individual waves should merge into one wave, the shape, position and kinetic parameters of which are determined by the first electron transfer step in the sequence [17,19]. The formal redox potential of this step, Eq. (11), accompanied by the activationless formation of a thermodynamically significant di-thallium(II) intermediate, Eq. (8),

can be defined as [11]:

$$E_1 = E_1^0 + \frac{RT}{F} \ln \left(\frac{[Tl^{III}(CN)_2{}^+]}{[Tl_2^{4+}]^{1/2}} \right). \quad (11)$$

3.4. Microscopic reversibility of the two-equivalent process

The overall mechanism of two-equivalent reduction of $[Tl^{III}(CN)_2]^+$ represented by Eqs. (8)–(10) implies that, analogously to the reduction process of $[Tl^{III}(aq)]^{3+}$, all three steps including two electrode and one chemical, presumably take place at the outer Helmholtz plane (OHP), as can be normally expected for strongly solvated redox-active ions [6,11]. According to the principle of microscopic reversibility, for the reverse oxidation process of $[Tl^{I}(aq)]^+$ to $[Tl^{III}(aq)]^{3+}$ (or to $[Tl^{III}(CN)_2]^+$, vide infra) one can expect the following common starting steps [11]:

$$2\,[Tl^{I}(aq)]^+ - 2e^- \Rightarrow 2\,[Tl^{II}(aq)]^{2+} \quad \text{(slow)} \quad (12)$$

$$2\,[Tl^{II}(aq)]^{2+} \Rightarrow [Tl^{II} - Tl^{II}]^{4+} \quad \text{(fast)} \quad (13)$$

The estimated standard potential for this reaction is ca. 1.5 V [11,28]. In fact, no anodic wave due to this process was detected within the potential range of 1.0–1.5 V, in the absence or presence of cyanide ions (Ref. [11] and the present work). The most probable reason for this observation is a violation of the principle of microscopic reversibility due to the essential asymmetry in the solvation features of reactant and product species. According to Koper and Schmickler [6], for soft and easily desolvable univalent ions such as $[Tl^{I}(aq)]^+$, the more probable redox path implies an ion transfer to the electrode followed by a strong specific adsorption on the electrode as a rate-determining step:

$$[Tl^{I}(aq)]^+ - \delta e^- \Rightarrow Tl(ads)^{(1+\delta)} \quad \text{(slow)} \quad (14)$$

$$Tl(ads)^{(1+\delta)} - (1-\delta)e^- \Rightarrow Tl^{II}(ads)^{2+} \quad \text{(slow)} \quad (15)$$

In this case, the $Tl^{II}(ads)^{2+}$ ion formed as an intermediate, is probably trapped in a local potential minimum on the electrode surface. This would shift the standard reduction potential to much higher value ($E_2^0 \geq 2$V) compared to that expected for the hypothetical (microscopically reversible) pattern, Eqs. (12) and (13). Unfortunately, studies in this potential range are complicated by the processes of oxygen evolution and formation of oxide films.

3.5. Other cyano-complexes of Tl^{III}

According to the established equilibrium relationships for the complexation between $[Tl^{III}]^{3+}$ and CN^- [13], at the concentrations of NaCN below or higher the frames quoted above, mostly the mixtures of other thallium cyanocomplexes, viz.: $[Tl^{III}(CN)]^{2+}$ and $[Tl^{III}(CN)_3]^0$ together with the already characterized compound $[Tl^{III}(CN)_2]^+$ can be formed. Formation of compound $[Tl^{III}(CN)_4]^-$ at nearly 100% content can be expected at the concentrations of NaCN exceeding 0.15 M (at otherwise similar conditions). The reduction wave for latter specie was found to overlap strongly with one belonging to the reduction of Tl^+ (unavoidably present in the solution), and hence has not been investigated in detail due to this complication. We were not able to disclose the reduction waves of two other species, $[Tl^{III}(CN)]^{2+}$ and $[Tl^{III}(CN)_3]^0$ in a whole range of available NaCN concentrations. The only observed well-defined wave in the presence of NaCN was proven to belong to the $[Tl^{III}(CN)_2]^+$ complex with the peak intensity corresponding to its molar fraction in the solution, calculated according to [13].

3.6. Reduction of $[(CN)_5Pt^{II}-Tl^{III}]^0$ ("compound I")

We have obtained also preliminary results for the electrochemical reduction of this long-lived bi-nuclear cyano-complexes at nearly saturating concentration of 10^{-3} M, 0.1 M in $HClO_4$ (no salt added). The cyclic voltammograms display two cathodic waves at ca. 0.3 and −0.3 V, Fig. 5, which can be ascribed to the manifestation of stepwise reduction of this compound ("compound I", according to the classification of Ref. [19,20]) by two electrons. These waves have no anodic counterparts even if the scan is reversed before reaching potentials where the Tl^{I} deposition begins. This mechanism is confirmed by formation of Tl^+ ions detected by appearance of characteristic $Tl^+ + e^- \Leftrightarrow Tl^0$ reduction and oxidation waves gradually increasing in intensity in the course of repetitive cycling (note that no Tl^+ ions were present in the starting solution), Fig. 5. We propose the following mechanism for the two step reduction of compound I:

$$[(CN)_5Pt^{II} - Tl^{III}]^0 + e^- \Rightarrow [(CN)_5Pt^{II} - Tl^{II}]^{\bullet -} \quad (16)$$

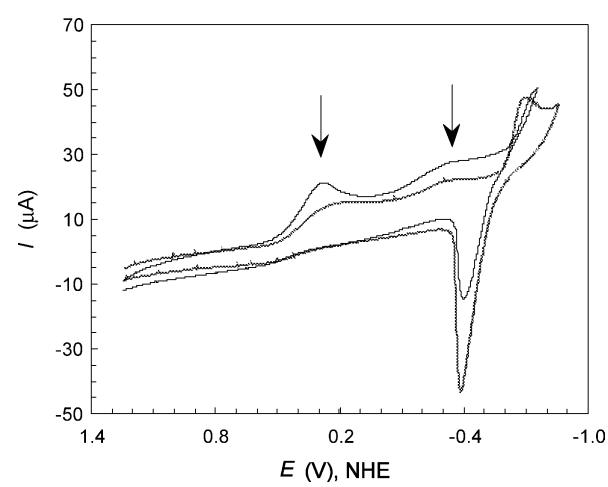

Fig. 5. Cyclic voltammograms for glassy carbon electrode (area: 0.0314 cm^2) in the solution: 0.001 M $[(CN)_5Pt^{II}–Tl^{III}]^0$ + 0.01 M $HClO_4$; bold curve: first cycle; gray curve: sixth cycle; scan rate $v = 0.1\ V\,s^{-1}$.

$$[(CN)_5Pt^{II} - Tl^{II}]^{\bullet -} + e^- \Rightarrow [Pt^{II}(CN)_4]^{2-} + Tl^+ + CN^- \quad (17)$$

(We note that the $[Pt^{II}(CN)_4]^{2-}$ complex is not electrochemically active within the potential range of +0.8 to −0.8 V, unpublished results). In contrast to the above considered cases of mononuclear thallium(III), in the absence or presence of cyanide ions, the electrochemical steps now seemingly have the reverse order of formal redox potentials (i.e. here $E_1^0 > E_2^0$) leading to the appearance of two cathodic waves [24,27].

4. Conclusions

For acidified solutions of $Tl^{III}(ClO_4)_3$, containing sodium cyanide at appropriate concentrations, in the potential range of +1.7 to −0.7 V, the only electro-active particles are $[Tl^{III}(CN)_2]^+$ and $[Tl^{III}(CN)_4]^-$. The reduction wave for the latter complex occurs at the potentials, where reduction of $[Tl^I]^+$ (present in the working solutions as an impurity), also takes place. Reduction of thallium(III) (present as $[Tl^{III}(CN)_2]^+$) to $[Tl^I(aq)]^+$, as in the case of reduction of $[Tl^{III}(aq)]^{3+}$, goes through the quasi-simultaneous sequential mechanism, provided that the transfer of the first electron is rate-determining step. So, the overall mechanism of two-equivalent reduction does not change upon the complexation with cyanide, though the parameters do change for the kinetically significant first (slow) step. The second step should be identical in the presence and absence of cyanide ions in the solution. Presumably the difference between standard potentials of first and second electron transfer steps both in the presence and absence of NaCN is more than 180 mV ($E_2^0 > E_1^0$) and, consequently, one can observe only a single combined (merged) reduction wave (see also Ref. [11]).

Preliminary results for the electrochemical two-equivalent reduction of the novel di-nuclear long-lived compound $[(CN)_5Pt^{II}–Tl^{III}]^0$ also indicate the two-step mechanism, but, obviously, in contrast to the above-mentioned cases of reduction of mononuclear thallium(III), the steps have the reverse order for standard redox potentials ($E_1^0 > E_2^0$) leading to the appearance of two separated cathodic waves.

In closing we would like to mention that the two-electron mechanisms proposed above, especially conclusion about the involvement of a Tl(II) dimer as an intermediate, require further justifications by using of additional approaches and/or techniques. A significant extension of this work is planned with the application of a high scan rate cyclic voltammetry, in the combination with a methodology of modification of electrodes by the self-assembled monolayer films of different composition and thickness (for illustrative cases, see Refs. [29,30]). The latter approach, potentially allowing for the prevention of direct interaction of reactant ions with the electrode surface, and, hence, for an exclusion of otherwise unavoidable adsorbed states, seem to be extremely promising regarding the redox couples under the present interest.

Acknowledgements

The continuous support from the Swedish Natural Sciences Research Council (NFR) and the European Commission through INTAS Project No. 96-1162 are kindly acknowledged. The authors are grateful to Dr. E. Ahlberg for introducing them to the CVSIM program and helpful discussions.

References

[1] R.K. Clayton, Photosynthesis. Physical Mechanisms and Chemical Patterns, Cambridge University Press, Cambridge, 1980.
[2] D.S. Bendall (Ed.), Protein Electron Transfer, BIOS Scientific Publication, Oxford, 1996.
[3] P.E.M. Siegbahn, M.R.A. Blomberg, Chem. Rev. 100 (2000) 421.
[4] D. Uhrhammer, F.A. Schultz, J. Phys. Chem. A 106 (2002) 1630.
[5] L.D. Zusman, D.N. Beratan, J. Phys. Chem. A 101 (1997) 4136.
[6] M.T.M. Koper, W. Schmickler, J. Electroanal. Chem. 450 (1998) 83.
[7] E.G. Petrov, Ya.R. Zelinskyy, V. May, J. Phys. Chem. B 108 (2004) 13208.
[8] A.G. Lee, The Chemistry of Thallium, Elsevier, Amsterdam, 1971, Chapter 9.
[9] J. Glaser, Adv. Inorg. Chem. (1995) 43.
[10] M.I. Bellavance, B. Miller, in: A.J. Bard (Ed.), Encyclopedia of Electrochemistry of the Elements, Marcel Dekker, New York, 1975, vol. IV, Chapter 4.
[11] D.E. Khoshtariya, T.D. Dolidze, L.D. Zusman, G. Lindberg, J. Glaser, Inorg. Chem. 41 (2002) 1728.
[12] E. Penna-Franca, R.W. Dodson, J. Am. Chem. Soc. 77 (1955) 2651.
[13] I. Blixt, B. Györi, I. Glaser, J. Am. Chem. Soc. 111 (1989) 7784.
[14] D.K. Gosser, A General Simulation Program (CVSIM), VCH, New York, 1993.
[15] R. Dronskowski, A. Simon, Angew. Chem. Int. Ed. 28 (1989) 758.
[16] S. Henkel, K.W. Klenkhammer, W. Schwarz, Angew. Chem. Int. Ed. 33 (1994) 681.
[17] W.C. Ermber, Y.S. Lee, K.S. Pitzer, J. Chem. Phys. 70 (1979) 293.
[18] D.A. Kleier, W.R. Wadt, J. Am. Chem. Soc. 102 (1980) 6909.
[19] M. Maliarik, K. Berg, J. Glaser, M. Sandsröm, I. Tóth, Inorg. Chem. 37 (1998) 2910.
[20] M. Maliarik, J. Glaser, I. Tóth, M.W. da Silva, L. Zékány, Eur. J. Inorg. Chem. (1998) 565.
[21] M. Maliarik, J. Glaser, I. Tóth, Inorg. Chem. 37 (1998) 5452.
[22] R. Greef, R. Peat, L.M. Peter, D. Pletcher, J. Robinson, Instrumental Methods in Electrochemistry, Southampton Electrochemistry Group, Horwood, New York, 1986, Chapter 6.
[23] R.S. Nicholson, I. Shain, Anal. Chem. 36 (1964) 706.
[24] A.J. Bard, L.R. Faulkner, Electrochemical Methods. Fundamentals and Application, Wiley, New York, 1980, Chapter 6.
[25] A.W. Bott, Curr. Separat. 16 (1997) 61;
A.W. Bott, Curr. Separat. 18 (1999) 9.
[26] L.I. Krishtalik, Double Layer and Electrode Kinetics (in Russian), Nauka, Moscow, 1981, Chapter 5 (p. 198–282).
[27] D.S. Polcyn, I. Shain, Anal. Chem. 38 (1966) 370.
[28] N. Hush, Trans. Faraday Soc. 57 (1961) 557.
[29] D.E. Khoshtariya, T.D. Dolidze, L.D. Zusman, D.H. Waldeck, J. Phys. Chem. A 105 (2001) 1818.
[30] T.D. Dolidze, D.E. Khoshtariya, D.H. Waldeck, J. Macyk, R. van Eldik, J. Phys. Chem. B 107 (2003) 7172.